3.3 INVESTIGATION OF CARBON MONOXIDE IN THE CITY OF SÃO PAULO USING LARGE EDDY SIMULATION

Georgia Codato[a1], Amauri P. de Oliveira[a], Jacyra Soares[a],
Edson P. Marques Filho[b] and Umberto Rizza[c]

[a]Group of Micrometeorology, University of São Paulo, SP, Brazil.
[b]Federal University of Rio de Janeiro, Rio de Janeiro, RJ, Brazil.
[c]Istituto di Scienze dell'Atmosfera e del Clima, Lecce, Italy.

1. INTRODUCTION

One of the most important consequences of the urbanization is the increase in the number of vehicles and, consequently, in the emission of pollutants in the atmosphere (Table 1).

The city of São Paulo (Fig. 1), with about 11 millions habitants, together with 39 other smaller cities, forms the Metropolitan Region of São Paulo (MRSP). This region, located about 60 km far from the Atlantic Ocean, is occupied by 20.5 millions of habitants and has approximately 7 millions of vehicles. The MRSP has an area of 8,051 km^2 and it is the largest urban area in South America and one of the 10 largest in the world (Codato *et al.,* 2007).
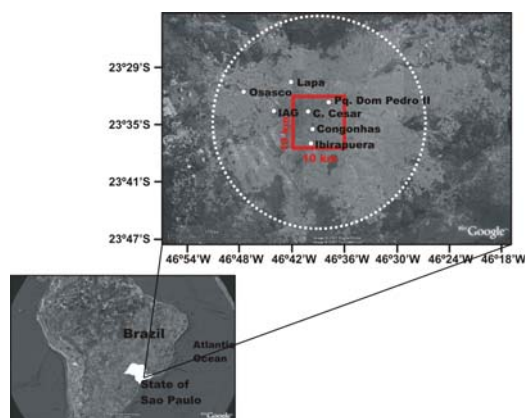

FIG. 1. Geographic position of the Metropolitan Region of São Paulo. The red square indicates the LES horizontal domain. Large circle indicates the traffic area limit used to estimate the advecção in the region.

The MRSP has emitted about 1,460,000 ton of carbon monoxide per year (CETESB, 2006). Approximately 97% of this emission is due to 7 million vehicles, and under low wind conditions a considerable fraction of carbon monoxide (CO) remains in the metropolitan area generating highly concentrations in the regions of intense traffic.

Air pollution is the most important environmental problem in São Paulo. There are indications that long term exposure to high levels of pollutants has caused dramatic public health problems (Martins *et al.*, 2002 and Novaes *et al.*, 2007). There are also evidences that pollution in São Paulo has even altered the local climate by affecting the diurnal evolution of diffuse, direct and global solar irradiance components at the surface locally (Oliveira *et al.*, 2002) and in regional scale (Codato *et al.,* 2007).

Table 1. Annual emission of CO in mega cities.			
Place	Latitude, Longitude and altitude	Habitants and vehicles (million)	Tg of CO per year
São Paulo, Brazil. (CETESB, 2006)	23º33'S, 46º44'W, 742m	20.5/7	1.48
México City, México. (Gurjar and Lelieveld, 2005)	19º36'N 98º57'w, 2240m	18.1/*	1.8
New York, USA. (EPA, 1997)	40º47'N 73º58'W, 30.5m	8.1/*	3.0
Los Angeles, USA. (EPA, 1997)	36º03'N 118º14'W, 233m	11.8/*	3.6
Moscow, Russian. (Gurjar and Lelieveld, 2005)	55º46'N 37º40'E, 150m	10.4/ 2.7**	1.3
Shanghai, China. (Gurjar and Lelieveld, 2005)	31º13'N 121º28'E, 4m	18 / 1[&]	2.2
Beijing, China. (Gurjar and Lelieveld, 2005)	39º54'N 116º23'E, 43m	17/ 3[$]	2.7
* Not available;** http://mos.ru/wps/portal/ [&]http://www.shanghai.gov.cn [$]http://www.chinadaily.com.cn			

The objective of this work is to investigate the statistical properties of the convective planetary boundary layer (PBL) over a homogeneous urban surface using the large eddy simulation model

---

[1] Corresponding author address: Departamento de Ciências Atmosféricas, IAG, USP, Rua do Matão 1226, 05508-090, São Paulo, SP, Brazil. Email: georgia.codato@terra.com.br.

(LES) developed by Moeng (1984). Here, special attention will be given to the characterization of the turbulent transport of carbon monoxide at the top of the PBL during daytime.

2. CARBON MONOXIDE AT THE SURFACE

The observations of CO concentration displayed here (Figs. 2 and 3) were carried out by the air quality monitoring network of São Paulo State Environmental Protection Agency (CETESB, 2006) between 1996 and 2005. The station geographic positions are indicated in Table 2.

Table 2. Meteorological and air pollution stations.

Station	Localization (Lat, Long)	Height (m)	Parameter Mesured
IAG	23°33'34''S, 46°44'01''W	742	M
C. Cesar	23°33'11''S 46°40'20''W	817	CO
Congonhas	23°36'57''S 46°39'46''W	760	CO
Ibirapuera	23°35'30''S 46°36'43''W	750	CO and W
Pq. Dom Pedro II	23°32'40''S 46°37'45''W	730	CO and W
Lapa	23°30'32''S 46°42'04''W	720	CO and W
Osasco	23°31'34''S 46°47'29''W	740	CO and W
M stands for meteorological parameters; **CO** for CO concentration and **W** for wind speed and direction.			

Observations have indicated that the CO concentration in São Paulo presents a maximum during winter (June-August) and a minimum during summer (Fig. 2). The CO horizontal variability can be associated to the regional distribution of vehicle traffic (Fig. 1).
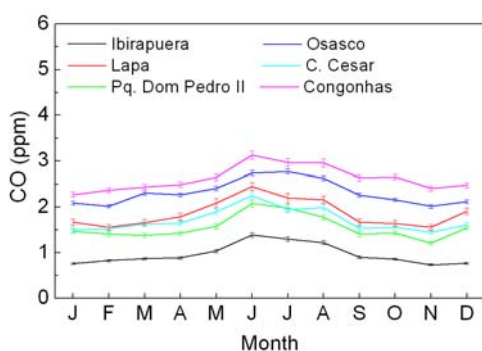

FIG. 2. Seasonal evolution of monthly averaged CO concentration at the surface in São Paulo. Data from 1996 to 2005.

Small values of CO occur in Ibirapuera because this station is located inside a highly forested park with small traffic of vehicles. Higher values of CO in Osasco and Congonhas are due to the fact these stations are located adjacent to heavy traffic roads. The other stations (Lapa, C. Cesar and Pq. Dom Pedro II) show an intermediate behavior.

The diurnal evolution of monthly averaged values of CO (Fig. 3) observed during June (highest concentration period in São Paulo) indicated similar spatial pattern. The progressive decreasing of CO concentration at the surface level at the end of nighttime, reaching a minimal (0.26-0.45 ppm) around 05:30 LT (local time), is a common feature to all stations. The first maxima occur between 08:30 LT and 09:30 LT in most of the stations. The second maxima occurs between 19:30 and 21:30 LT. The second minima occur between 14:30 and 16:30 LT in all stations.
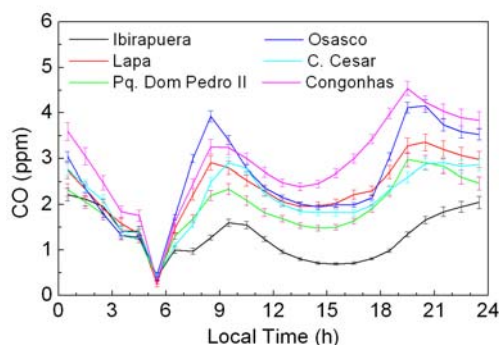

FIG. 3. Diurnal evolution of monthly averaged values of CO concentration at the surface in São Paulo during June. Data from 1996 to 2005.

The diurnal evolution of CO concentration at the surface in MRSP is due to: (i) surface emission associated to the intense traffic of vehicles; (ii) entrainment in the top of the PBL of clean air and (iii) horizontal advection of clean air from not urban areas.

3. WIND AT THE SURFACE

The wind pattern in the MRSP shows spatial variations due to the difference in the land use and due to topographic effects (Oliveira *et al.*, 2003). Fig. 4 indicates that in average the wind speed in Lapa and Osasco is twice the value in Ibirapuera. Pq. Dom Pedro II shows an intermediate behavior.
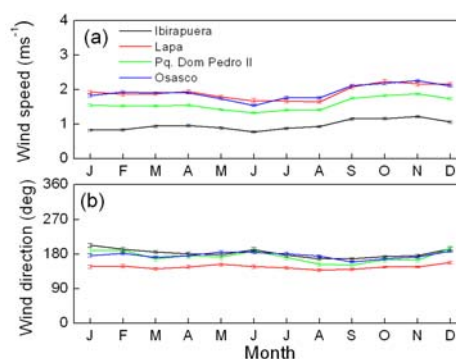

FIG. 4. Seasonal evolution of monthly averaged (a) wind speed and (b) wind direction at the surface in São Paulo. Data from 1996 to 2005.

Similar spatial variation is found in the diurnal evolution of the wind at the surface during June in MRSP (Fig. 5). In average the wind speed during daytime is almost twice larger than during

nighttime. The systematic shift from East to South in the afternoon indicates the presence of sea breeze. Besides sea breeze, there are observations evidences that the patterns of low-level circulation in the MRSP are also strongly affected by local topography and landuse. These local effects are present even during June (winter) in São Paulo, as observed previously by Oliveira *et al.* (2003).
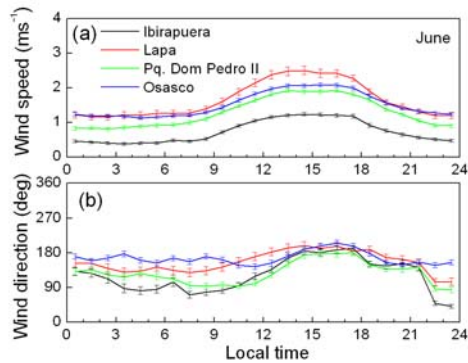

FIG. 5. Diurnal evolution of monthly averaged (a) wind speed and (b) wind direction at the surface in São Paulo during June. Data from 1996 to 2005.

Despite low intensity, the winds in São Paulo contribute to reduce the concentration of CO by advecting clean not-urban air from uptown (outside area of the circle of Fig. 1). It is possible to estimate the intensity of clean air advection considering that not urban values of CO in São Paulo are equal to 0.2 ppm (Granier, 1996) and using the monthly average values of CO and wind speed estimated in each station (Table 3). The horizontal advection is removing CO in all investigated stations (Fig. 1). In average over all stations, horizontal advection removes about 0.4 ppm per hour.

Table 3. Horizontal advection of CO in June.

Station	$|\vec{V}|$ (km h^{-1})	$|\nabla_H CO|$ (ppm km^{-1})	$\partial CO/\partial t$ (ppm h^{-1})
C. Cesar	2.67	0.05	-0.14
Congonhas	4.66	0.08	-0.39
Ibirapuera	6.00	0.10	-0.61
Pq. Dom Pedro II	5.49	0.11	-0.63
Lapa	4.71	0.09	-0.44
Osasco	2.67	0.05	-0.14
Average	4.66	0.08	-0.39

The diurnal evolution of the horizontal advection in June over MRSP was estimated considering the monthly averaged hourly values of CO and the horizontal wind speed spatially averaged over the domain (Fig. 6). Advection is always removing CO from MRSP, contributing with most of the cleaning during nighttime. After 05:00 LT the vehicle emissions control the evolution of CO concentration in MRSP yielding a rates of 1 ppm h^{-1}. After the early morning increase the vertical evolution of the PBL begins to contribute to the

daytime evolution of CO, reducing surface values of CO by vertical mixing.

Considering the idealized diurnal evolution of CO flux, based on vehicles traffic inventory (Marques Filho, 2004), it is possible conclude that the decreasing in the CO concentration after 10:00 LT may be related to the entrainment of clean air in the top of the PBL. Therefore, this work will investigate how the entrainment of clean air in the top of the PBL during the time that the PBL reaches its maximum vertical evolution - around noontime - affects the observed CO concentration decreasing at the surface.
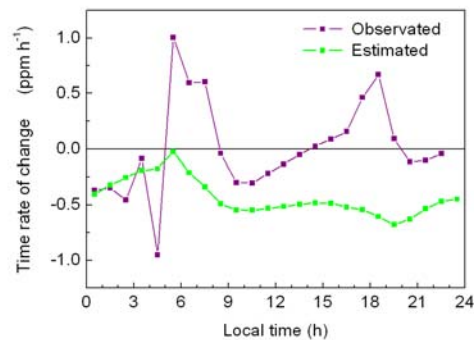

FIG. 6. Diurnal evolution of monthly averaged time rate of change for CO observed at the surface in São Paulo and estimated from horizontal advection, both during June. Data from 1996 to 2005.

4. NUMERIC MODEL

The numerical simulation of turbulent flows is carried out in LES solving directly the large eddies (resolved-scale). The small-scale part of the turbulent flow (subgrid-scale) is solved indirectly by parameterization techniques. This LES version was developed by Moeng (1984).

The LES code has been used by the Group of Micrometeorology in the University of São Paulo to simulate the PBL properties for highly convective conditions (Marques Filho, 2004) and to investigate the pollution dispersion by considering a continuously emitting area and point sources located at the surface (Marques Filho *et al.*, 2007).

The numerical simulations in this work were carried out using a parallel version of the LES code. It was run in a cluster with 32 nodes of the Laboratory of Computation at the University of São Paulo (LCCA-USP).

4.1. Initial and boundary conditions

The domain used in the numerical simulation was formed by 128 by 128 by 128 grid points in x, y and z, respectively, covering 10 km by 10 km by 2 km (Fig. 1).

The model was run for 5 hours, corresponding to 6,000 time steps. In the simulations carried out here the time step was around 1 second, corresponding to about 5 hours of PBL time evolution. It required about 210 hours of CPU time in the cluster.

The initial conditions for pollutant concentration and potential temperature correspond to a mixed layer with vertical extension of 300 m (Fig. 7). The initial mixed layer potential temperature and pollutant concentration was respectively 290 K and 2.5 ppm. Above 300 m the potential temperature increases about 9 K in the inversion layer, assumed 100 m thick. In the free atmosphere, the lapse was set constant and equal to 5 K km^{-1}. The vertical variation of CO concentration in the inversion layer is equal to 2.3 ppm. In the free atmosphere above the inversion layer the CO concentration was assumed constant and equal to 0.2 ppm, a not-urban value of CO concentration for the region (Granier *et al.,* 1996). The vertical profiles of horizontal velocity components (u, v) are assumed to be constant and equal, respectively, to a zonal geostrophic wind of 5 m s^{-1} and zero (Fig. 7).
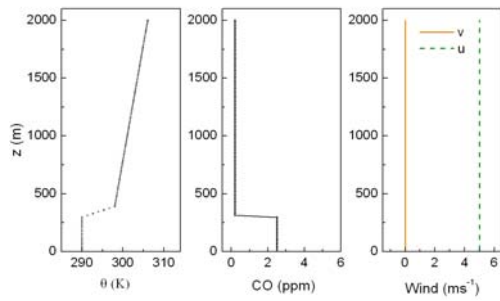

FIG. 7. Initial conditions for potential temperature carbon monoxide and wind speed components.

The diurnal evolution of the sensible heat flux at the surface was assumed as a sine function of the local time with maximum amplitude equal to 250 W m^{-2} at 12 LT (Fig. 8). This corresponds to about 30% of the global solar radiation observed under clear sky conditions during the winter in the city of São Paulo (Marques Filho, 2004).
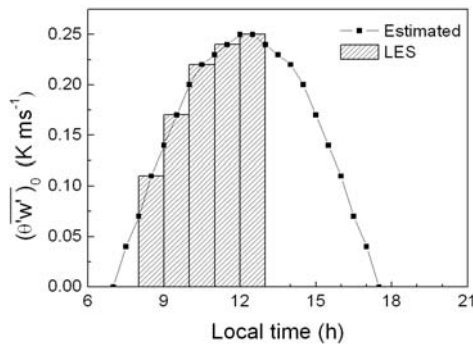

FIG. 8. Diurnal evolution of sensible heat flux at the surface used as boundary condition in the LES model. Columns indicate that during each one hour the flux used in the LES was kept constant. Fluctuation of potential temperatura and vertical velocity are indicated by θ´ and **w**´, respectively. Reynolds averaged is indicated by $\overline{(\ \ )}$.

The diurnal evolution of the carbon monoxide flux at the surface was assumed to vary with time according to:

$$\overline{(c'w')}_0 = \frac{B_{CO}}{\sigma_t \sqrt{2\pi}} \left[e^{-\frac{1}{2}\left(\frac{t-t_{01}}{\sigma_t}\right)^2} + e^{-\frac{1}{2}\left(\frac{t-t_{02}}{\sigma_t}\right)^2} \right] \quad (1)$$

where B_{CO} is the amplitude (μg m^{-2}), σ_t is the standard deviation (s), t is local time (s) and t_{01} and t_{02} are the local time (s) of the maximum flux. Expression (1) corresponds to the bimodal behavior of the vehicles traffic in urban areas, with a maximum at $t=t_{01}$ and $t=t_{02}$.

To estimate the amplitude of CO flux at the surface it was considered the total emission of CO in the MRSP equal to 1.48 million of tons per year divided by number of days in one year and by the area representative traffic in São Paulo (8,051 km^2 according to CETESB, 2006). The amplitude of CO flux, B_{CO}, is estimated by imposing the following relation:

$$B_{CO} = \int_0^{24\,hours} \overline{(c'w')}_0 \, dt = 0.50 \times 10^6 \ \mu g\,m^{-2} \quad (2)$$

The relation proposed by Seinfeld (1988, page 7) was used to convert μg m^{-3} into ppm considering the temperature and atmospheric pressure constant and equal to 290 K and 930 mb, respectively.

Two maximum amplitude of the carbon monoxide vertical flux, at the surface, of about 1.26 ppm m s^{-1} (or 13.95 μg m^{-2} s^{-1}) were set at t_{01}=36000 s (10:00 LT), t_{02}= 86400 s(19:00 LT) and σ_t = 7200 s. The amplitude of the surface flux of CO used in the simulation is indicated in the Fig. 9.
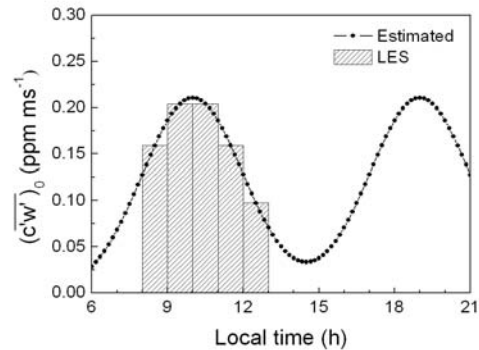

FIG. 9. Diurnal evolution of CO turbulent flux at the surface, used as boundary condition in the LES model. Columns indicate that during each one hour the flux used in the LES was kept constant. Fluctuation of CO concentration and vertical velocity are indicated by **c**´ and **w**´, respectively. Reynolds averaged is indicated by $\overline{(\ \ )}$.

It should be emphasized that the flux of CO indicated in Fig. 9 is the one used in the simulation described here. This flux is about 6 times smaller than the one estimated from the CO year inventory from Environmental Protection Agency (CETESB, 2006).

The reason for this discrepancy is because the flux based on the inventory yields unrealistic

values of CO concentration in the simulation using LES. It is not clear why this discrepancy had happen. One possibility is that the horizontal advection of less polluted air from outside the urban area compensates the intensity of the vehicle emission. Another possibility is that the inventory provide by protection agency is not right.

The aerodynamic roughness parameter is set equal to 0.16 m, corresponding to the urban value of roughness (Marques *et al.*, 2007).

These conditions were defined in order to simulate the time evolution of PBL during daytime in a realistic but simple way.

4.2. Spin up

During the spinup time (3600 time steps) ithe sensible heat and the carbon monoxide fluxes at the surface are kept constant and equal to 0 K m s^{-1} and 0 ppm m s^{-1}.

4.3. Quasi-steady equilibrium

The turbulent flow in PBL reaches a quasi-steady equilibrium when its properties vary with a time scale smaller than the time scale of the boundary conditions and external forcing variations. Under this condition, the PBL statistical properties can be determined as a function of the PBL characteristic scales, which in turn are defined as a function of the boundary conditions, external forcing and the intrinsic turbulent flow characteristics (Sorbjan, 1986). In Fig. 10, after the initial jump, PBL turbulence simulated by LES reaches the quasi-steady equilibrium around 1000 s of simulation time.
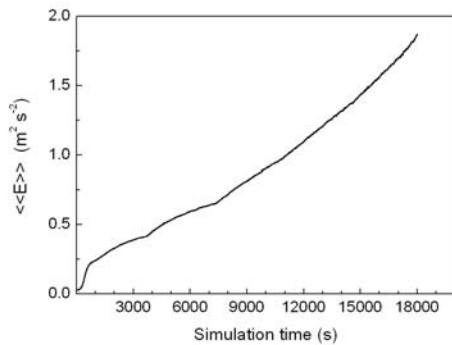

FIG. 10. Time evolution of turbulent kinetic energy per unit of mass (TKE) volume-averaged in the PBL. Volume-averaged values are indicated by << >>. The TKE (E) is estimated as 0.5 (u'^{2}+v'^{2}+w'^{2}).

5. RESULTS

The results presented hereafter are based on the three-dimensional fields generated during an interval of 1200 time steps (approximately 20 minutes). The statistics were obtained using 10 model outputs separated by 120 time steps each, corresponding to 20 minutes average. The statistical properties are estimated at 8:30, 9:30,

10:30, 11:30 and 12:30 LT after PBL has reached a state of quasi-equilibrium (Fig. 10).

The Obukhov length (L), PBL height (z_i), stability parameter ($-z_i/L$) and the characteristic scales of velocity (w_*) and time (t_*), simulated numerically by LES every 1 hour are indicated in Table 4. It is interesting to observe that during the five hours of simulation the stability parameter was within $12 \leq -z_i /L \leq 34$. Therefore the simulations correspond to typical convective conditions.

The vertical profiles of potential temperature, zonal component of wind, CO concentration and theirs respective vertical fluxes and variances, shown here, correspond to the ensemble average obtained from seven outputs, separated by 1200 time steps each. It is important to emphasize that the time step is approximately 1 second.

Table 4. PBL characteristic scales.					
Local time (h)	L (m)	z_i (m)	$-z_i/L$	w_* (m s^{-1})	t_* (s)
8.5	-24.7	328	14.2	1.08	318
9.5	-16.8	375	23.4	1.30	360
10.5.	-14.8	453	30.9	1.49	350
11.5	-16.0	593	32.6	1.60	380
12.5	-18.5	797	32.3	1.69	401

5.1. PBL evolution

Figure 11 indicates the vertical profiles of potential temperature and the respective vertical flux of sensible heat. It is possible to see the major features of a typical convective PBL, i.e. mixed layer with close to zero potential temperature vertical gradients and a linearly decreasing profile of sensible heat flux.
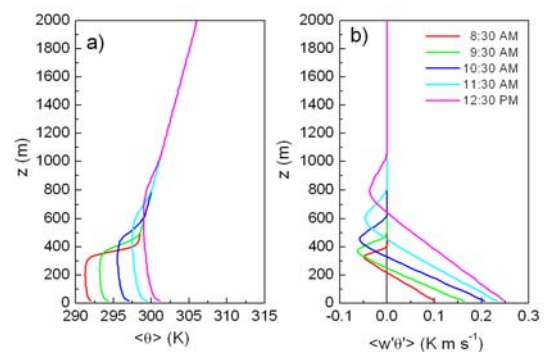

FIG. 11. Vertical profiles of (a) potential temperature and (b) sensible heat flux. Area-averaged values are indicated by < > and their respective statistical fluctuations are indicated by primes.

The behavior of the vertical profiles of zonal component of wind does not show the typical mixed layer character. On the contrary, zonal component varies significantly in the PBL during most of the time of the simulation (Fig. 12a).
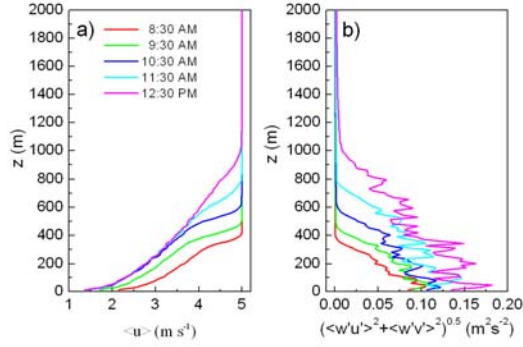
FIG. 12. Vertical profiles of (a) zonal component and (b) vertical flux of momentum. Symbols meaning are same as Fig. 11.

The vertical flux of horizontal momentum components shows a more complex variation with height (Fig. 12b). Vertical profiles of variance of horizontal (Fig. 13a) and vertical (Fig. 13b) components of wind behave as expected for convective conditions, with a maxima in the first one third of the PBL. The position of the maxima is consistent with the strong vertical shear present in the PBL (Fig. 12a).
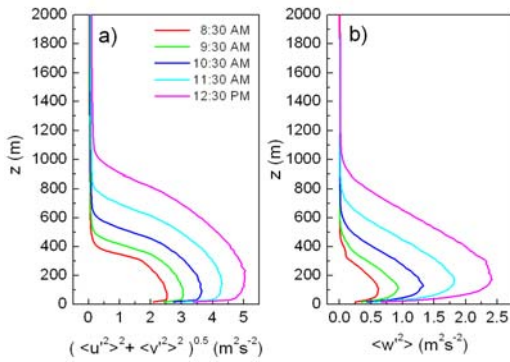

FIG. 13. Vertical profiles of (a) horizontal and (b) vertical wind speed variances. Symbols meaning are same as Fig. 11.

Vertical profile of CO concentration displays the typical mixed layer character (Fig. 14a). In association, the CO flux shows the characteristic linear variation with the height (Fig. 14b)

The time evolution of the CO concentration profiles indicate a progressive and persistent increasing during most of the morning due, exclusively, to the surface vehicular emission (Fig. 14a). During this period of time the vertical profiles of CO flux decreases linearly with height. Only around noontime the entrainment of clean air at the top of the PBL takes over the evolution of CO concentration in the mixed layer (Fig. 14a). In this case the vertical distribution of turbulent CO fluxes reflects this cleaning process undertaken by the PBL, with divergence flux in the entire PBL (Fig. 14b).

5.2. Entrainment

Entrainment due to penetrative convection is present during entire simulation period. After 5

hours the surface temperature modeled is larger than the observed one (Fig. 15). This indicates that the amplitude of the surface heat flux may be overestimated. It should be emphasized that the observations used in Fig. 15 correspond to monthly averaged hourly values based on 13 years of continuous observations in the IAG micrometeorological platform located at the University of São Paulo campus (Fig. 1, Table 2). There is also considerable entrainment of heat at the top of the PBL. The Ball ratio, defined as the ratio of flux at the top to the flux at the surface, is larger than 0.1 for heat flux (Fig. 16).
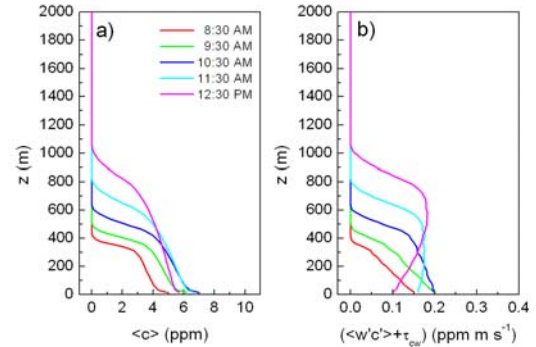

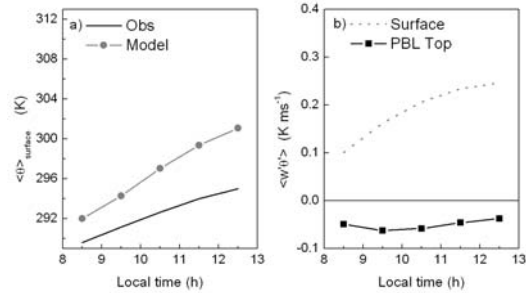**FIG. 14.** Vertical profiles of (a) CO mean values and (b) vertical CO flux. Symbols meaning are same as Fig. 11.

FIG. 15. Time evolution of simulated and observed (a) potential temperature and (b) vertical flux of sensible heat.
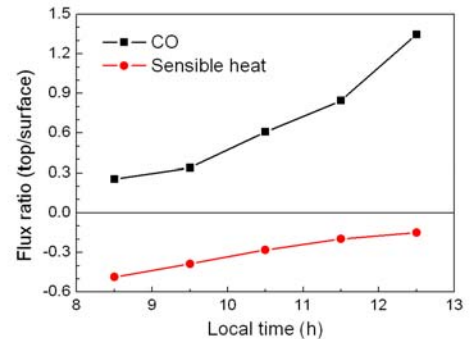

FIG. 16. Time evolution of the ratio of the turbulent flux top to the surface for CO and sensible heat modeled by LES. Symbols meaning are same as Fig. 11.

The time evolution of CO concentration shows large discrepancies between modeled and

observed values (Fig. 17a). Despite the strong entrainment at the top of the PBL (Fig. 17b) only after 10:30 LT the CO concentration in the PBL starts to decreases. The Ball ratio for CO flux indicates also values larger than 0.1 (Fig. 16).

5.3. Horizontal advection

The horizontal advection effect can be estimated by considering the horizontal wind speed in the model constant and equal to 18 km h^{-1}. This wind speed correspond to the initial condition (Fig. 7) and even tough the horizontal wind in the PBL varies during the simulation (Fig. 12) to simplify the analysis It will be considered constant and blowing from west. The horizontal advection is estimated by considering the CO concentration during June in the six stations (Fig. 1, Table 2). The horizontal gradient of CO was estimated considering the distance between stations and the west urban limit. Urban limit can be identified visually by the abrupt change in tons of grey, with white gray urban and dark grey not urban (Fig. 1).
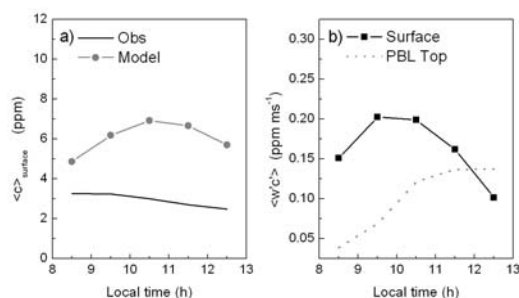

FIG. 17. Time evolution of simulated and observed (a) CO concentration and (b) vertical flux of CO.

The horizontal advection associated to the observed CO concentration and the wind speed used in the model is shown in Table 5. Taking into consideration the mean values it is possible to conclude that the hypothetical horizontal advection would contribute to reduced the discrepancies between the observed and modeled CO concentration.

Table 5. Horizontal advection of CO in June.

Station	$\left|\vec{V}\right|$	$\left|\nabla_H CO\right|$	$\partial CO/\partial t$
	(km h^{-1})	(ppm km^{-1})	(ppm h^{-1})
C. Cesar	18	0.10	-1.8
Congonhas	18	0.14	-2.5
Ibirapuera	18	0.06	-1.1
Pq. Dom Pedro II	18	0.06	-1.1
Lapa	18	0.11	-2.0
Osasco	18	0.16	-4.6
Average	18	0.11	-2.0

Figure 18 show the relative importance of all terms in the budget equation including the hypothetical horizontal advection.
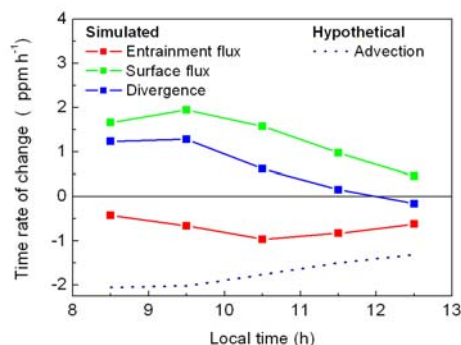

FIG. 18. Time evolution of the CO time rate of change associated to hypothetical horizontal advection, entrainment flux, surface flux and vertical divergence of the flux, simulated with LES.

6. CONCLUSION

Simulation of daytime evolution PBL over the MRSP carried out using LES model indicated several characteristics consistent with a convective PBL with significant contribution of mechanical production of TKE.

The simulated diurnal evolution of CO concentration indicates that entrainment of clean air at the top of the PBL is one of the dominant mechanism reducing the concentration of CO at the surface as observed in São Paulo even during the winter.

Comparison between entrainment, surface emission and hypothetical horizontal advection indicates that this late mechanism could be responsible by considerable reducing in the CO diurnal evolution in the city of Sao Paulo.

During this work, it was found an apparent discrepancy between the inventory emission proposed by CETESB and the diurnal evolution of CO in the MRSP (Table 1). The simulation carried here indicates the surface flux of CO must be at most 6 times smaller in order to generate CO concentrations similar to the observations. Next step would be evaluated the role of horizontal advection.

7. REFERENCES

CETESB (2006) Technical report on air quality in the State of São Paulo – Environmental State Secretary, ISSN 0103–4103, São Paulo, Brazil, 137pp. (*Available in Portuguese at http://www.cetesb.sp.gov.br*).

Codato, G., Oliveira, A.P., Soares, J, Escobedo, J.F., Gomes, E.N., and Pai, A.D., 2007: Global and diffuse solar irradiances in urban and rural areas in southeast of Brazil, *Theoretical and Applied Climatology* (*To be published*).

EPA, 1997: Determination of Annual Average CO Inventories and the Mobile Source Contribution in Selected Areas Using the 1990 OAQPS Trends Data Base. EPA-420-R-97-012.

Granier, C., Müller, J-F, Mandronich, S, Brassuer, G, 1996. Possible causes for the 1990-1993 decrease in the global tropospheric CO abundances: A three-dimensional sensitivy study. *Atmospheric Environment*, **30**, 1673-1682.

Gurjar, B.R., and Lelieveld, J., 2005: New Directions: Megacities and global change. *Atmospheric Environme*nt, **39**, 391-93.

Marques Filho, E.P., 2004: Investigação da CLP convectiva com modelo LES aplicado a dispersão de poluentes. PhD Thesis, Departamento de Ciências Atmosféricas, IAG-USP, 128 pp. (i*n Portuguese*)

Marques, E.P., Oliveira, A.P., Karam, H.A., and Rizza, U., 2006: Pollutant transport in a convective boundary layer with LES. *Brazilian Journal of Geophysics*, **24(4)**: 547-557.

Martins, L.C., Latorre, M.R., Saldiva, P.H., Braga A.L., 2002: Air pollution and emergency room visits due to chronic lower respiratory diseases in the elderly: na ecological time-series study in Sao Paulo, Brazil. *J. Occup. Environ. Med.,* **44(7**):622-627.

Moeng, C.A., 1984: Large-Eddy-Simulation Model for the Study of Planetary Boundary-Layer Turbulence. *Journal of the Atmospheric Sciences,* **41(13)**, 2052-2062.

Novaes, P., Saldiva, P.H., Kara-José, N, Macchione, M., Matsuda, M., Racca, L., and Berra, A., 2007: Ambient Levels of Air Pollution Induce Goblet Cell Hyperplasia in Human Conjunctival Epithelium. *Environmental health perspectives*, doi: 10.1289/ehp.10363 (available at http://dx.doi.org/).

Oliveira, A.P., Escobedo, J. F., Machado, A. J., and Soares, J., 2002: Diurnal evolution of solar radiation at the surface in the City of São Paulo: seasonal variation and modeling. *Theoretical and Applied Climatology*, **71(3-4)**, 231-249.

Oliveira, A.P.**,** Bornstein, R., and Soares, J., 2003: Annual and diurnal wind patterns in the city of São Paulo. *Water, Air and Soil Pollution: FOCUS,* **3,** 3-15**.**

Sánchez-Ccoyllo, O.R., Dias, P.L.S., Andrade, M.F., and Freitas S.R., 2006: Determination of O3-, CO- and PM10-transport in the metropolitan area of São Paulo, Brazil through synoptic-scale analysis of back trajectories. *Meteorol. Atmos. Phys.*, **92**, 83–93.

Seinfeld J.H, 1988: Atmospheric Chemistry and Phisycs of Air Pollution. *A Wiley Intersciences Puplication*, 738 pp.

Sorbjan, Z., 1986: On similarity in the atmospheric boundary layer. *Boundary-Layer Meteorology*, **35**, 377-397.